

On-line Distributed Model Predictive Scheduling for Multi-vehicle Routing Problems with Lane-change and Platoon Maneuvers

**Primary results about parameter sensitivity, scale robustness and
computational efficiency**

Authors: Nianhua Zhang, Fernando Viadero-Monasterio, Jicheng Chen, and Hui Zhang

0.1 Primary results about scale robustness

1. Basic 300-vehicle simulation explanation: The main reason for us to carry out several simulations with 300 vehicles is the practical configuration of CICT. As shown in Figure. 1, CICT has 104 self-owned vehicles and 184 other-owned vehicles. Considering the maximum number of vehicles including transportation units and social vehicles, 300 is set as the scheduled number of vehicles in our research. These data come from an organized investigation and discussion of the real-world scheduling environment in CICT. Therefore, we try to reproduce the practical condition for validation with the 300-vehicle configuration.

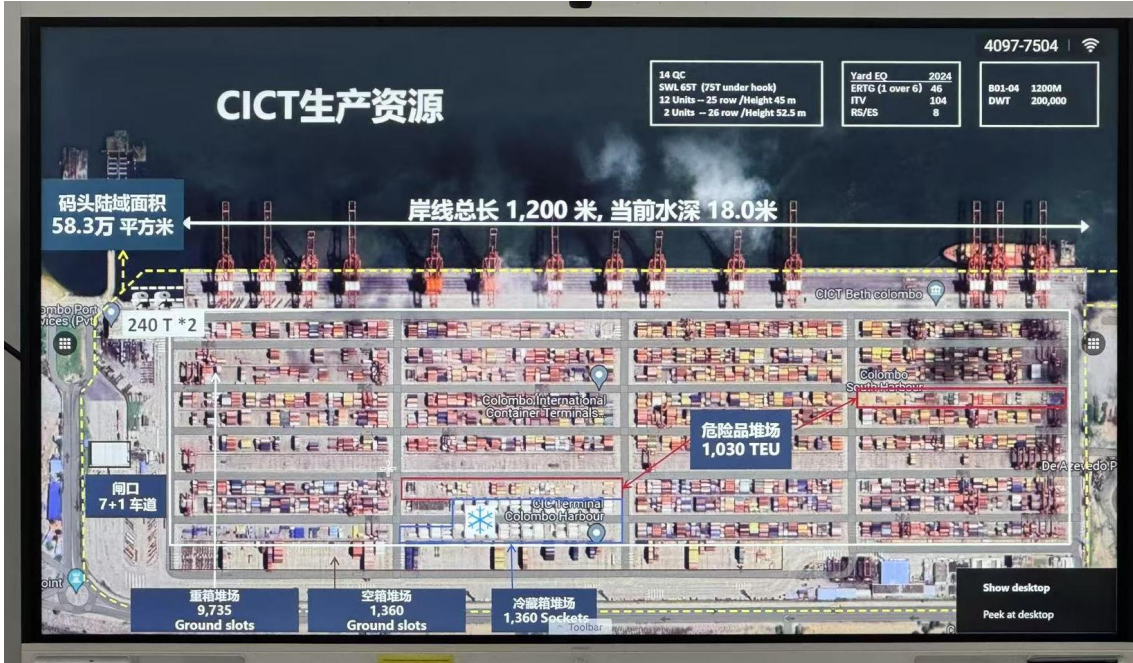


Figure 1: The overall operational conditions of CICT.

For robustness analysis, based on the practical information, we additionally introduce the simulations with 100 vehicles and 200 vehicles.

2. Extended 100-vehicle simulation results: For the 100 vehicles, the results are shown as following figures.

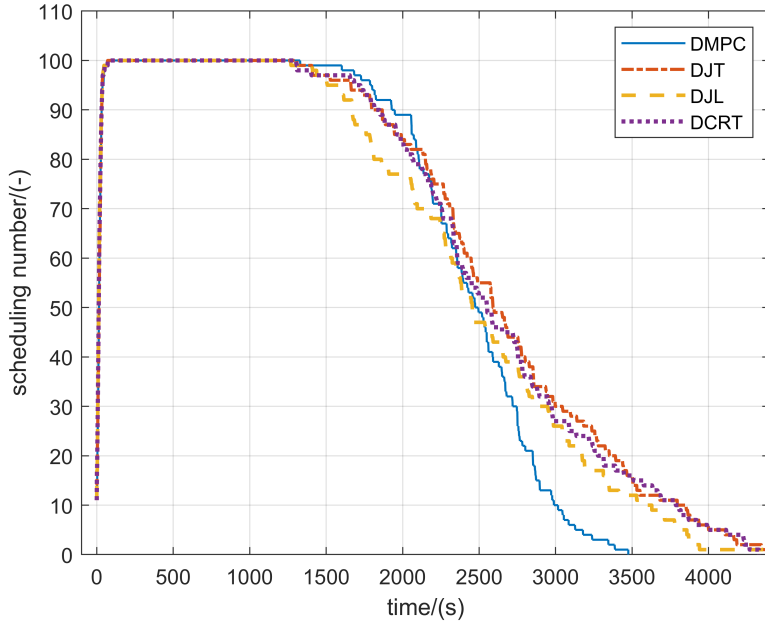


Figure 2: Scheduling vehicles in each dataframe.

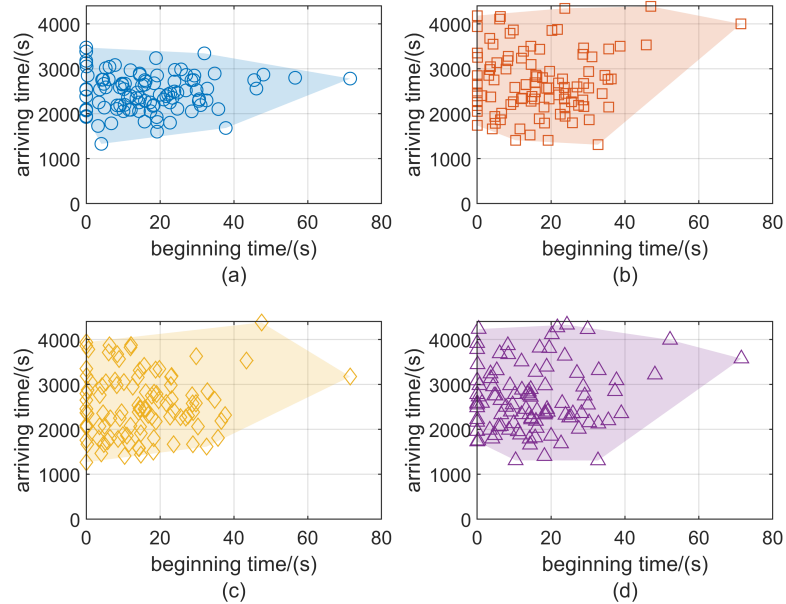


Figure 3: Entering and arriving time of vehicles: (a) DMPC (b) DJT (c) D JL (d) DRCT.

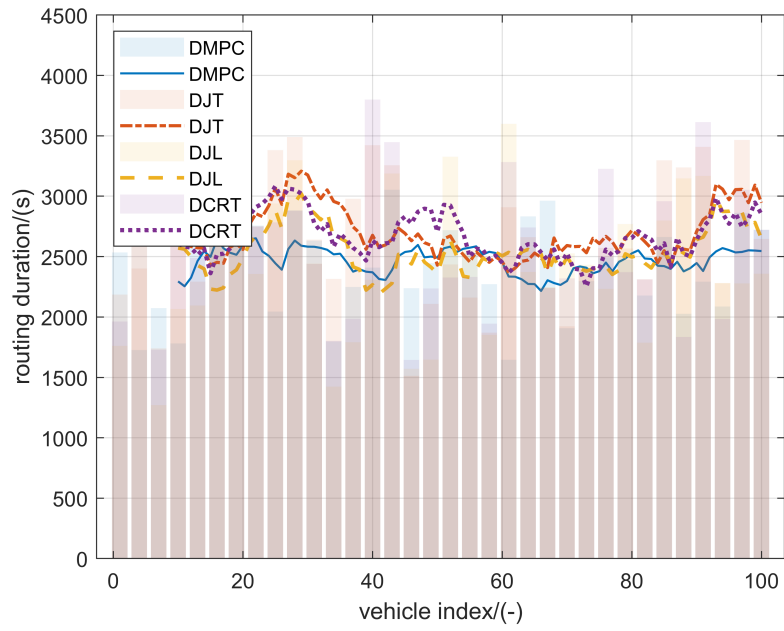


Figure 4: Routing duration of vehicles with different planners.

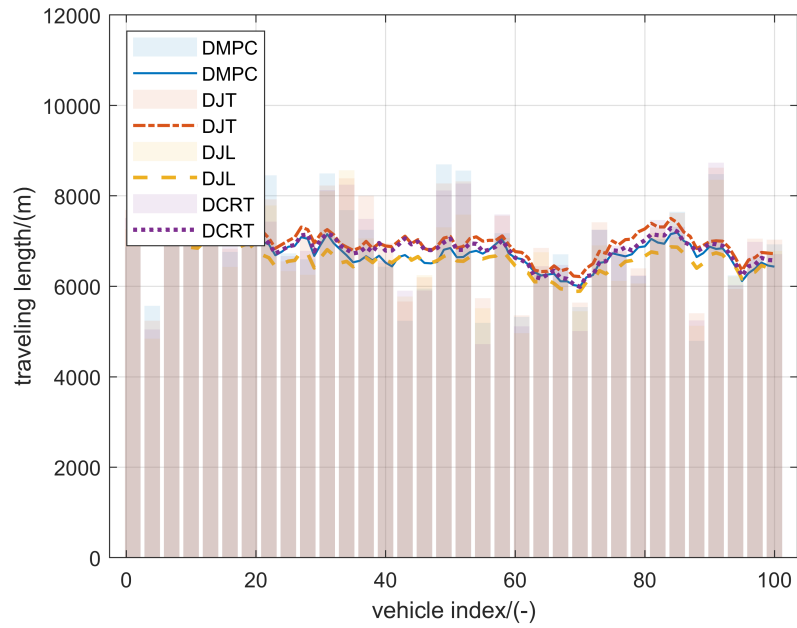


Figure 5: Traveling length of vehicles with different planners.

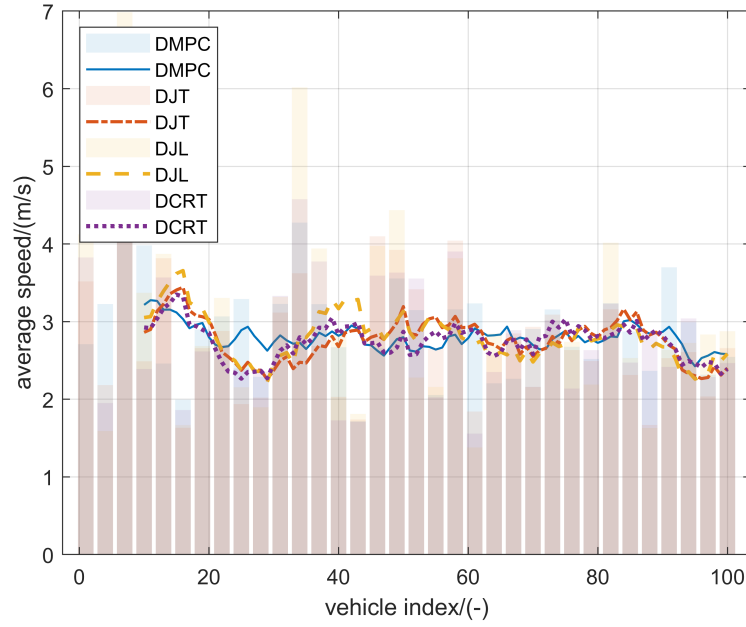


Figure 6: Average speed of vehicles with different planners.

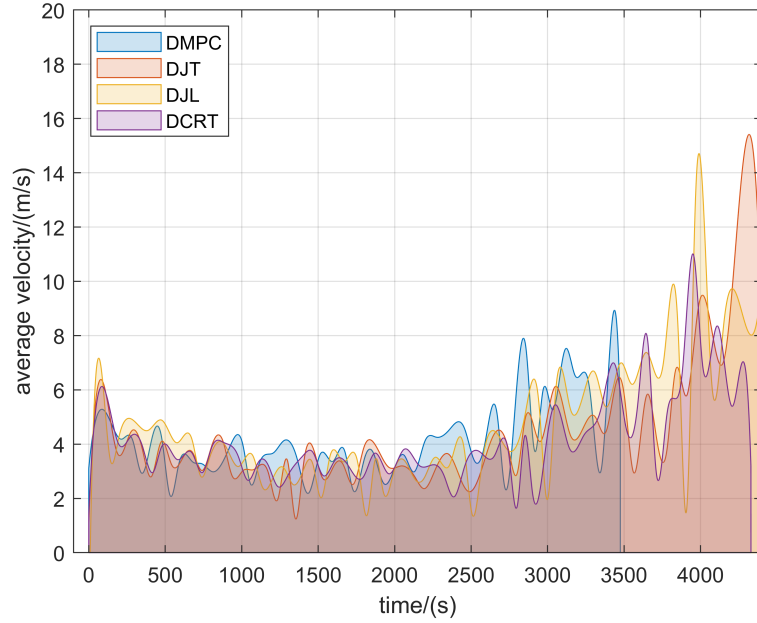


Figure 7: Average instantaneous speeds and envelopes for different planners.

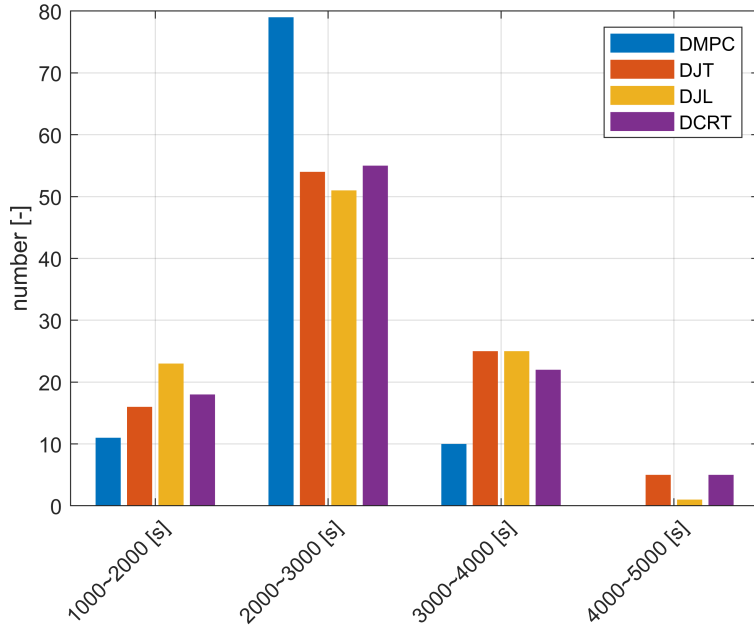


Figure 8: Distribution of routing duration with different planners.

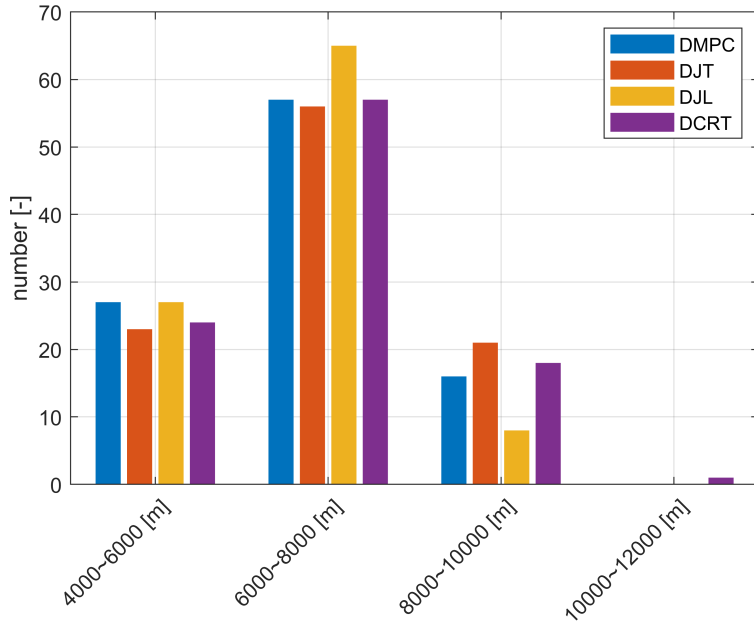


Figure 9: Distribution of traveling length with different planners.

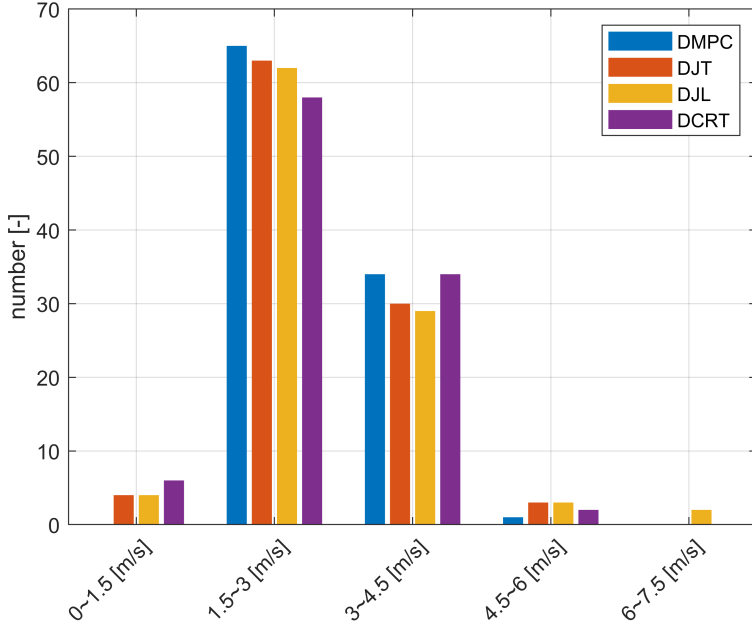


Figure 10: Distribution of average speed with different planners.

The 100-vehicle simulations are conducted within the 1st initialization in Table III of the manuscript. The results show a similarity to the presented 300-vehicle results. As shown in Fig. 2, the number of scheduled vehicles exhibits a rapid increase up to 100 and is followed by a gradual decline for the sequential entry and exit. DMPC demonstrates superior performance compared to others due to its precise forecasting capabilities and collaborative routing strategies. As shown in Fig. 3, the distribution of entering time and arriving time for vehicles are depicted within a phase plane. With the unified y-axis, the minimum arriving times for DMPC and others are relatively close, within 1500s. As shown in Fig. 4, the routing duration of DMPC is shorter than those of other planners. As shown in Fig. 5, the traveling lengths of different planners are relatively similar. As shown in Fig. 6, the average speed of the DMPC shows an improvement compared with other planners. As shown in Fig. 7, at the beginning and the end of the whole routing process, the average speed performs a high level with severe shaking, which follows the trend described in the manuscript. As shown in Fig. 8, for all 4 planners, the majority of vehicles complete their transportation tasks within a time frame between 2000 s and 3000 s. Notably, the DMPC planner facilitates a higher number of vehicles finishing their missions within 3000 s, and demonstrates superior time efficiency. As shown in Fig. 9, for all 4 planners, the majority of scheduled routes fall between 6000 m and 8000 m. As shown in Fig. 10, for the 3 planners excluding DMPC, most of vehicles perform their average speeds within 1.5-3 m/s, which is different from this (4-6 m/s) of the DMPC.

Quantitatively, similar numerical indicators are introduced in this paper as Table 1 to show the improvements of the DMPC. As shown in Table 1, the proposed DMPC demonstrates superior time efficiency. It is noticed that, for the DJL, though the average length is shorter and average velocity is higher, the overall scheduling time of 100 vehicles

Table 1: Quantified improvements with 100 vehicles.

Indicators	DMPC	DJT	DJL	DCRT
T_{end}	3475.0	4343.9	4333.4	4304.9
T_{ave}	2460.3	2696.6	2537.9	2661.9
L_{ave}	6736.6	6953.3	6562.1	6825.3
v_{ave}	2.8026	2.7614	2.8081	2.7437

(4333.4 s) is still longer than the DMPC (3475 s). It is an evidence for the nonnegligible influence caused by waiting for the traffic lights in time-efficient MVRP, which is one of the basic issues motivate us to introduce traffic lights.

2. Extended 200-vehicle simulation results:

Similarly, for 200 vehicles, simulations are carried out and the results are shown as following figures.

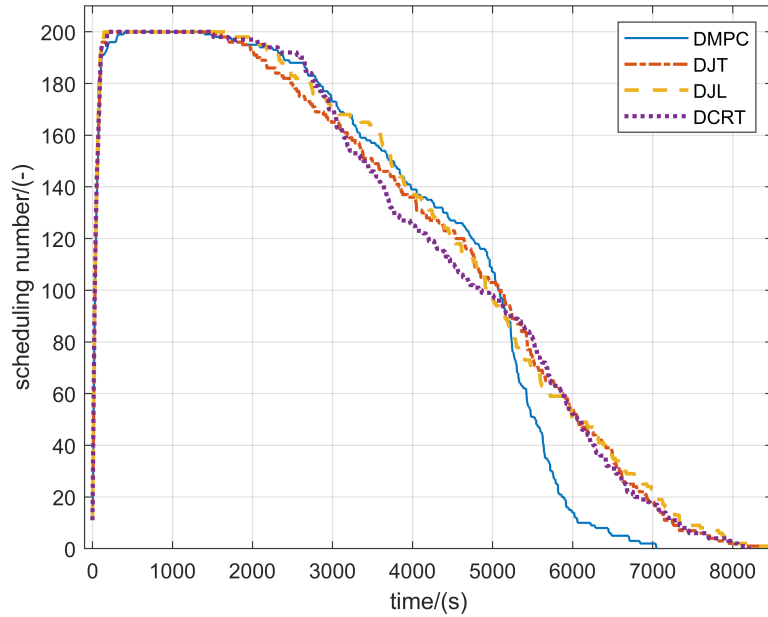


Figure 11: Scheduling vehicles in each dataframe.

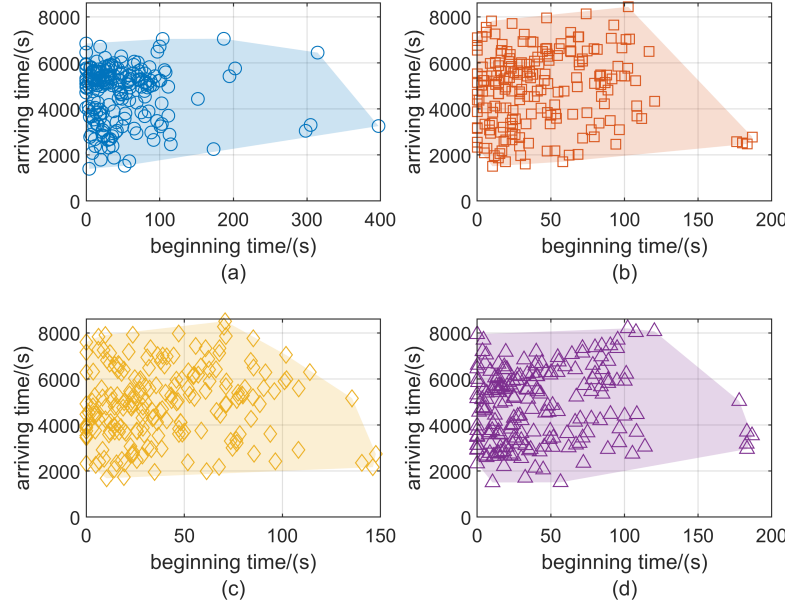


Figure 12: Entering and arriving time of vehicles: (a) DMPC (b) DJT (c) DJL (d) DRCT.

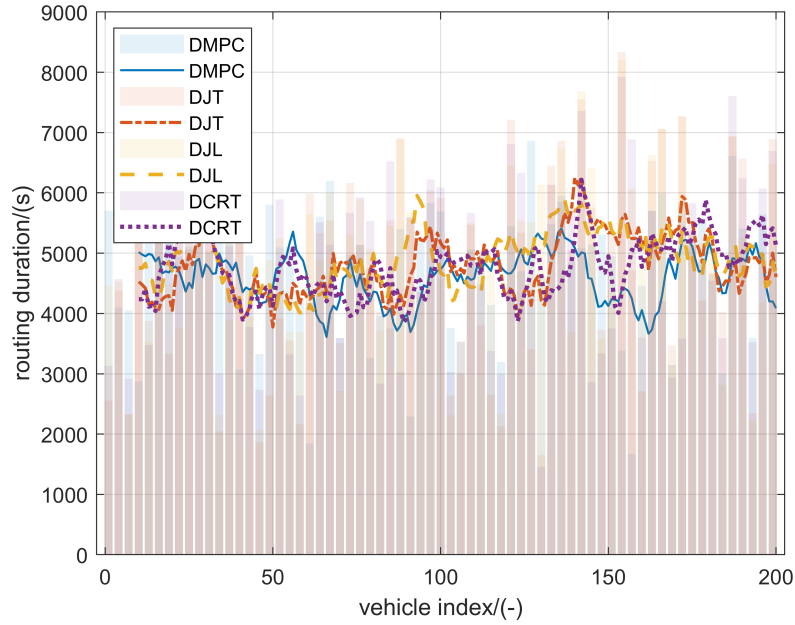


Figure 13: Routing duration of vehicles with different planners.

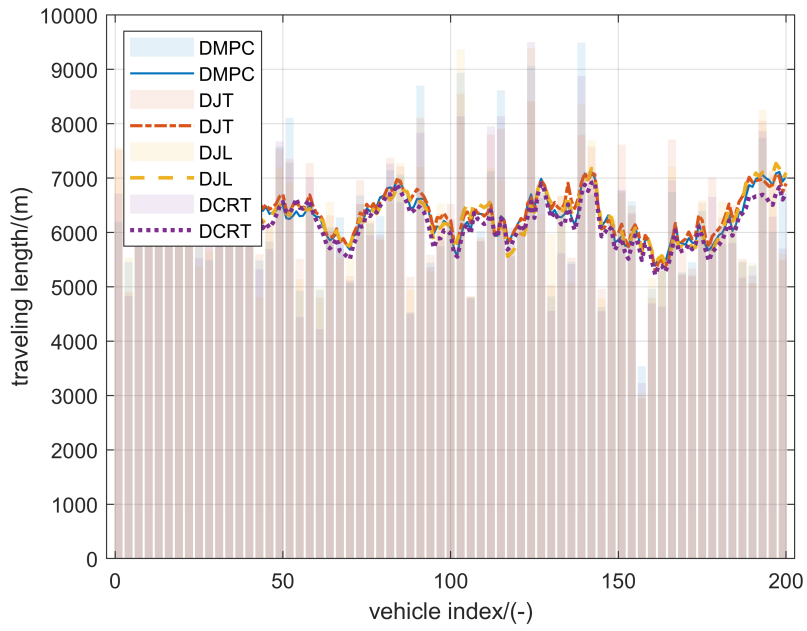


Figure 14: Traveling length of vehicles with different planners.

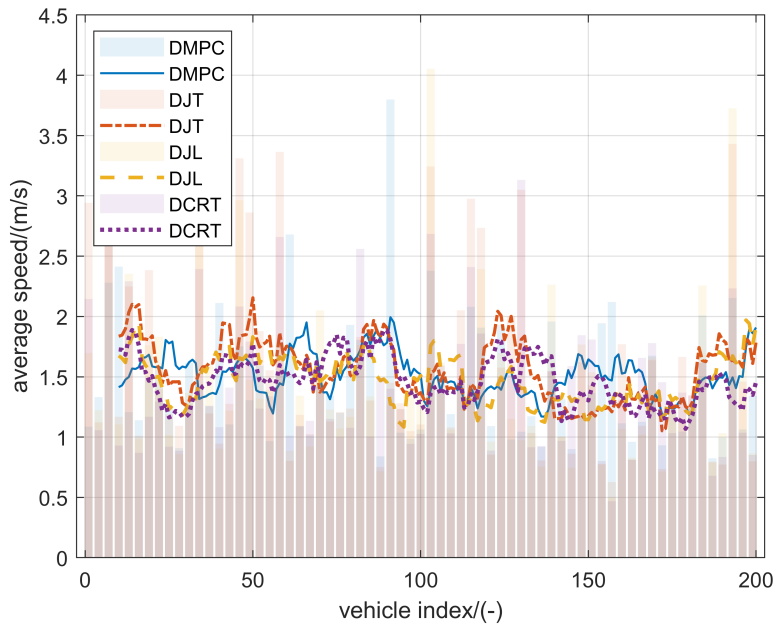


Figure 15: Average speed of vehicles with different planners.

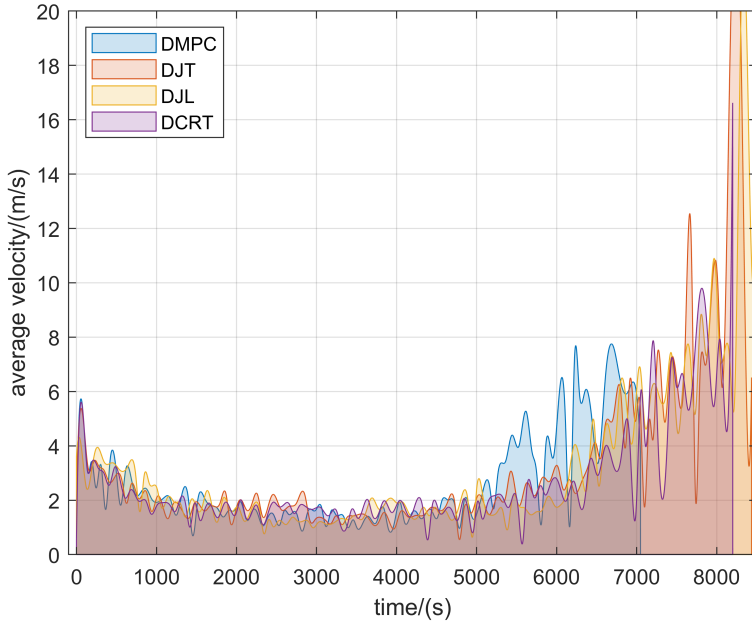


Figure 16: Average instantaneous speeds and envelopes for different planners.

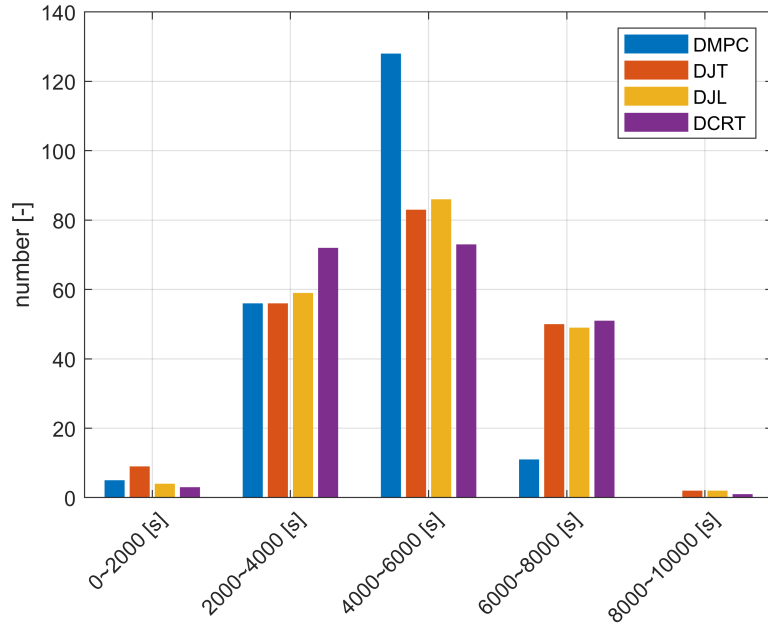


Figure 17: Distribution of routing duration with different planners.

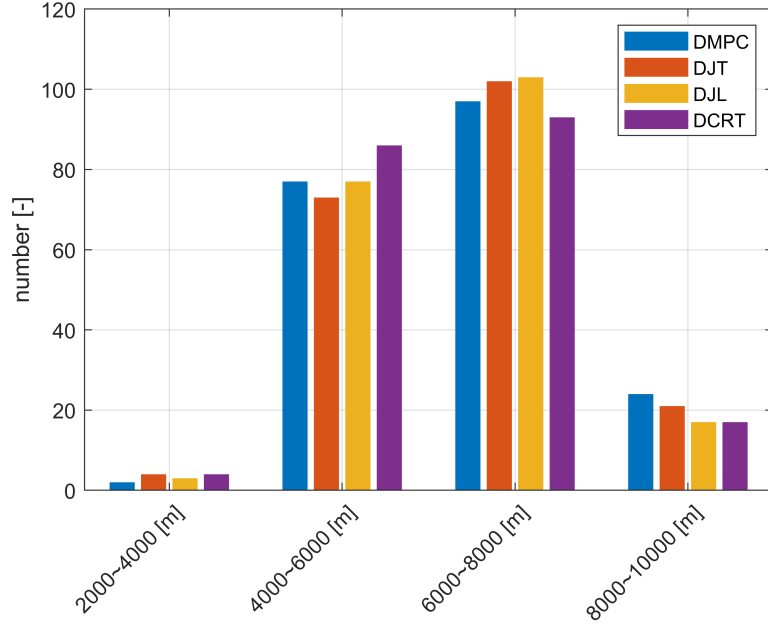


Figure 18: Distribution of traveling length with different planners.

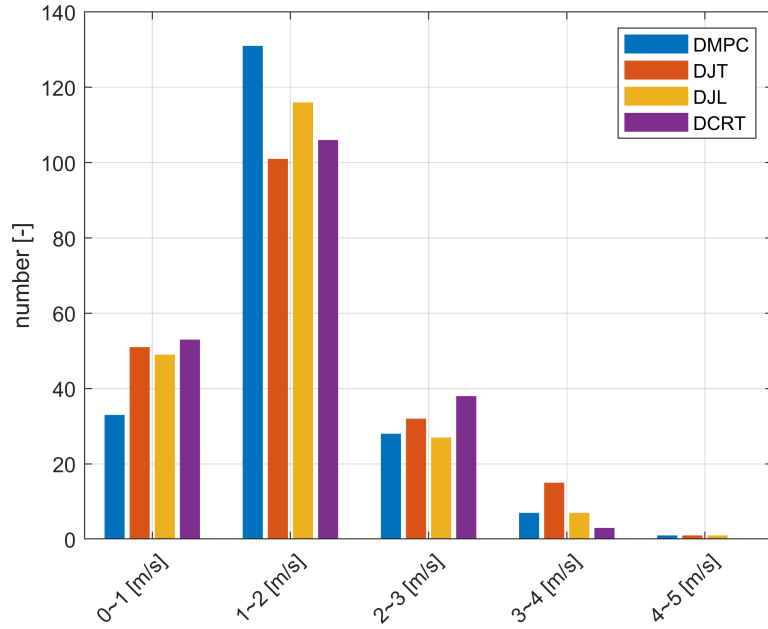


Figure 19: Distribution of average speed with different planners.

The results of 200-vehicle simulations show a similarity to the presented 300-vehicle results. As shown in Fig. 11, the number of scheduled vehicles exhibits a rapid increase up to 200 and is followed by a gradual decline, where the DMPC demonstrates superior performance compared to others. As shown in Fig. 12, the distribution of entering time

and arriving time for vehicles are depicted within a phase plane. With the unified y-axis, the minimum arriving times for DMPC and others are relatively close, within 2000 s. As shown in Fig. 13, the routing duration of DMPC is shorter than those of other planners. As shown in Fig. 14, the traveling lengths of different planners are relatively similar. As shown in Fig. 15, the average speed of the DMPC shows an improvement compared with other planners. As shown in Fig. 16, at the beginning and the end of the whole routing process, the average speed performs a high level with severe shaking, which follows the trend described in the manuscript. As shown in Fig. 17, for all 4 planners, the majority of vehicles complete their transportation tasks within a time frame between 4000 s and 6000 s. Notably, the DMPC planner facilitates a higher number of vehicles finishing their missions within 6000 s, and demonstrates superior time efficiency. As shown in Fig. 18, for all 4 planners, the majority of scheduled routes fall between 6000 m and 8000 m. As shown in Fig. 19, for all 4 planners, the majority of traveling velocities fall between 1.5 m/s and 2 m/s.

Quantitatively, similar numerical indicators are introduced in this paper as Table 2 to show the improvements of the DMPC. As shown in Table 2, the proposed DMPC

Table 2: Quantified improvements with 200 vehicles.

Indicators	DMPC	DJT	DJL	DCRT
T_{end}	6937.8	8332.7	8440.7	8097.6
T_{ave}	4604.8	4795.9	4872.0	4761.5
L_{ave}	6363.9	6406.2	6348.0	6202.4
v_{ave}	1.5165	1.5692	1.4884	1.4736

demonstrates superior time efficiency.

0.2 Primary results about parameter sensitivity

- Extracted parameters for sensitivity analysis:

For the parameters in Table I, d_α^{RSU} is defined to group \mathcal{G}_V , which will not directly affect the performance of routing. The control gains k^t, k^θ, k^d, k^v are calculated based on the H_∞ theory, which are designed based on our previous work[5]. k_N, k_L, k_T are the parameters introduced to generate the searching space \mathbf{G}_i , which is also designed based on our previous work[11]. Besides, based on [11], the prediction horizon N_p is set as 2 to balance the computing complexity and the performance. The inter-vehicle distance d^r and time headway h^r are also designed from our previous experience of platoon control[11, 12]. Therefore, we focus on the newly introduced parameters θ^r, v^r, k_Q, k_C to conduct the fundamental sensitivity analysis.

- Sensitivity analysis for v^r :

Extending the baseline $v^r = 15$ as $v^r = 10, v^r = 20, v^r = 25$, the sensitivity analysis are conducted with the 1st initial configuration in Table III. The results are shown from Figure. 20 to Figure. 28.

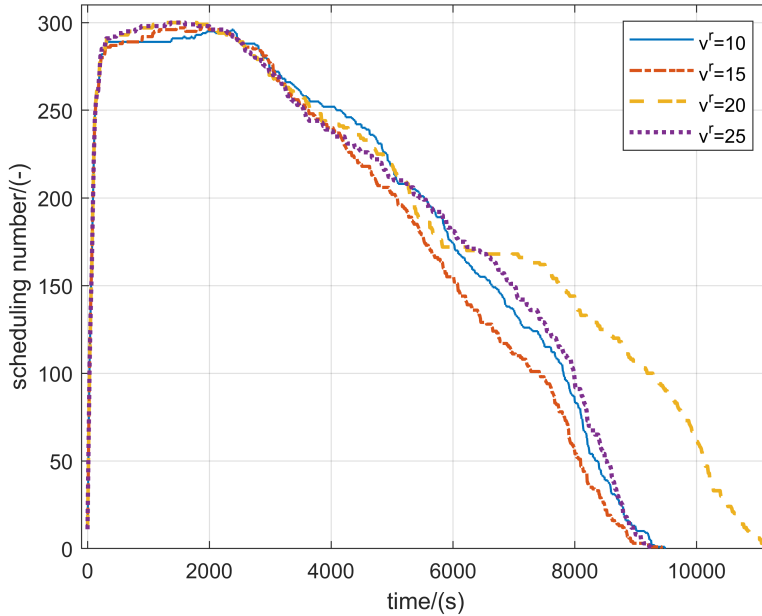


Figure 20: Scheduling vehicles in each dataframe.

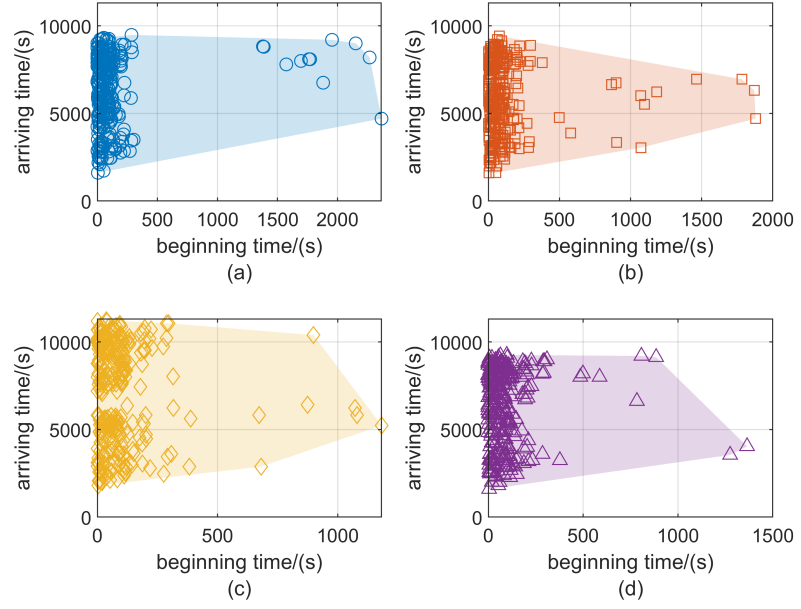


Figure 21: Entering and arriving time of vehicles: (a) $v^r = 10$ (b) $v^r = 15$ (c) $v^r = 20$ (d) $v^r = 25$.

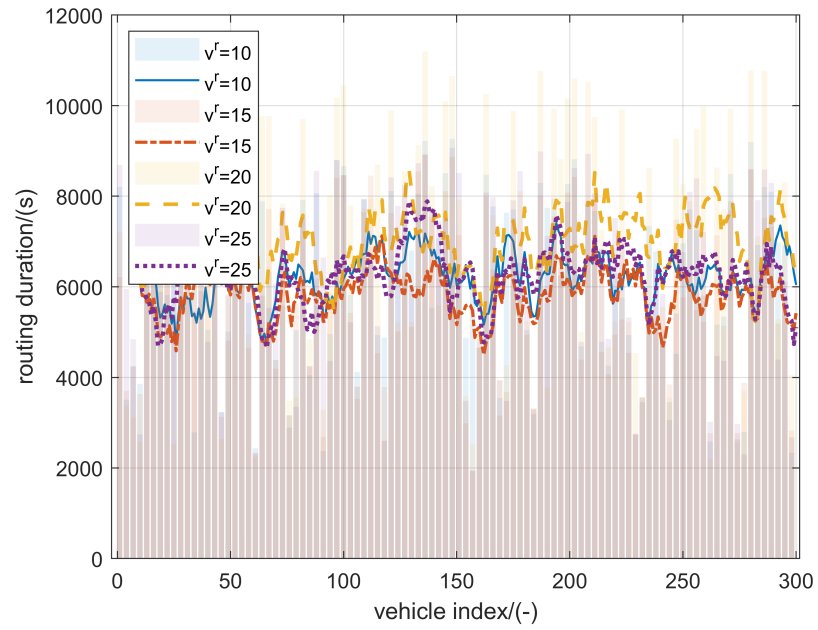


Figure 22: Routing duration of vehicles.

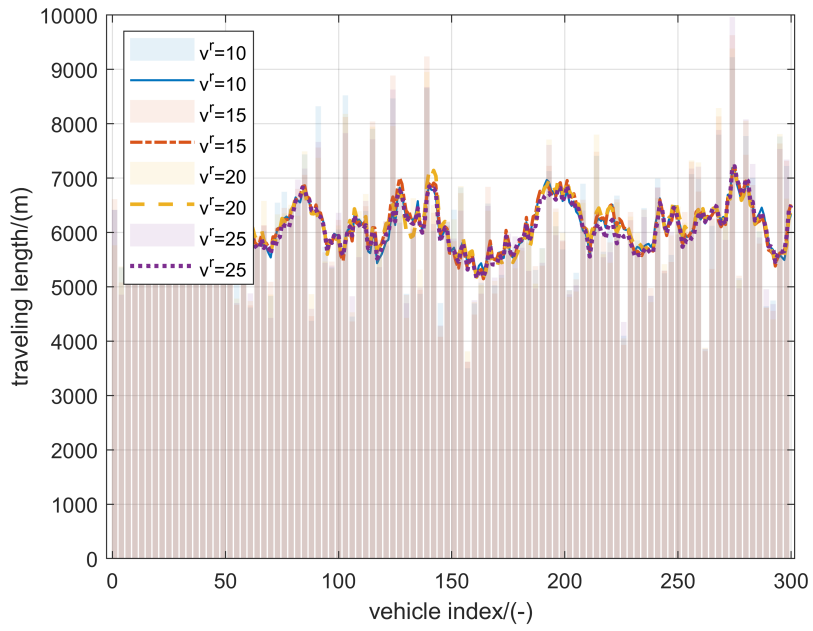


Figure 23: Traveling length of vehicles.

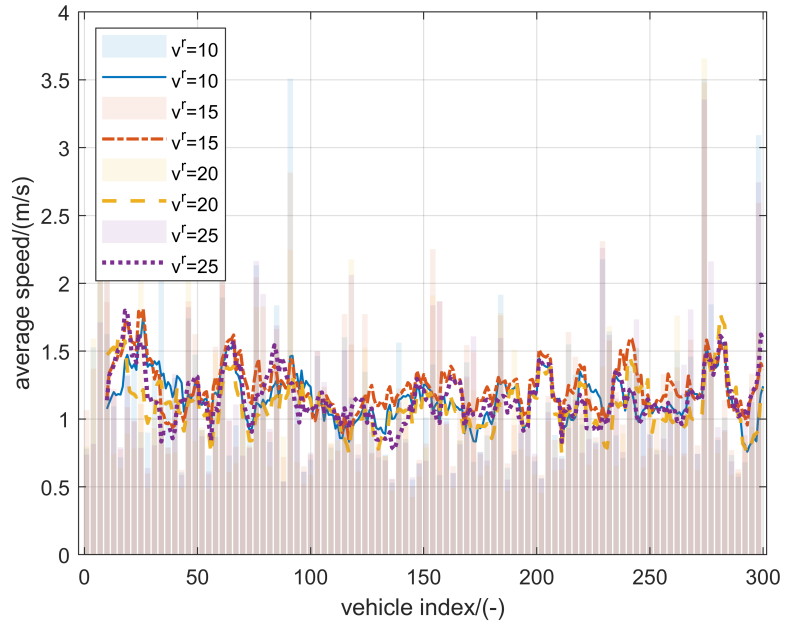


Figure 24: Average speed of vehicles.

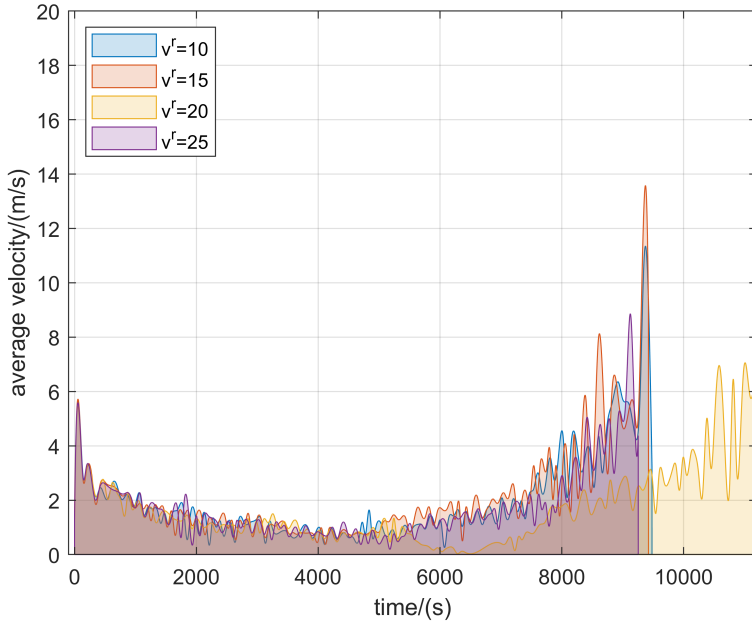


Figure 25: Average instantaneous speeds and envelopes.

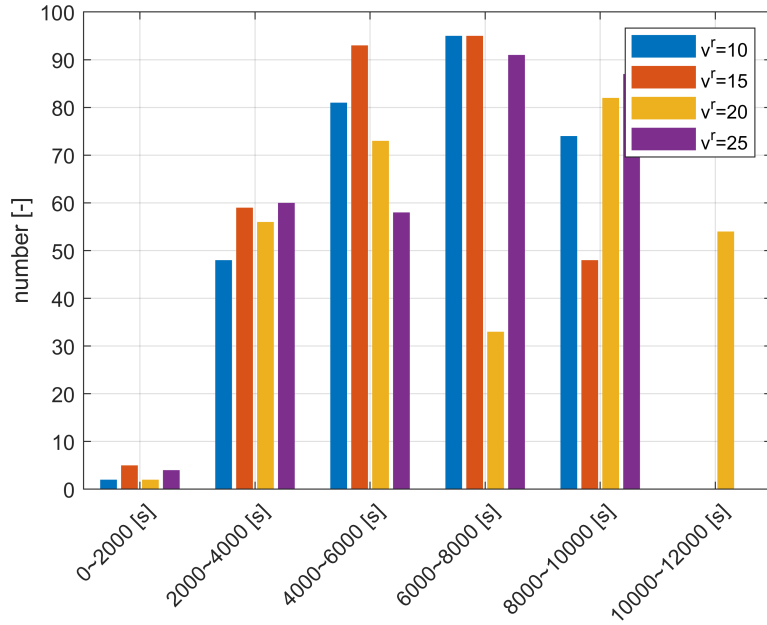


Figure 26: Distribution of routing duration.

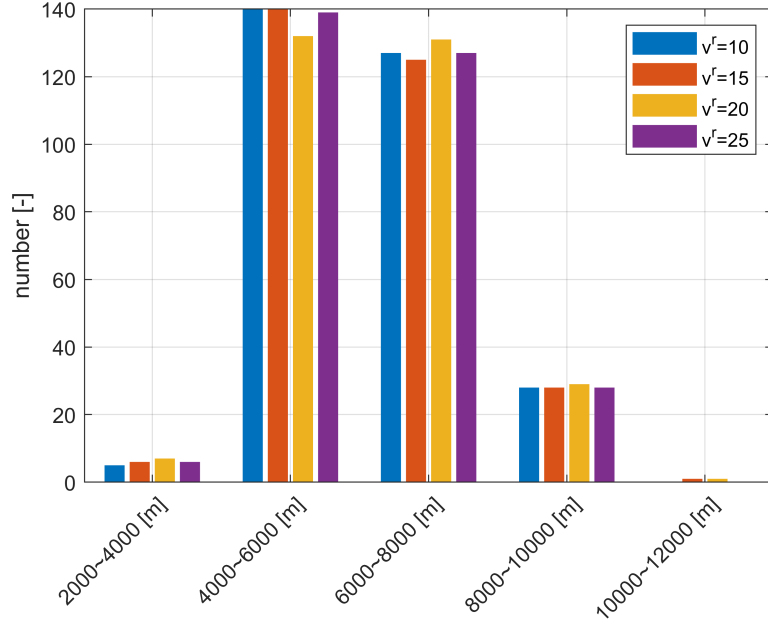


Figure 27: Distribution of traveling length.

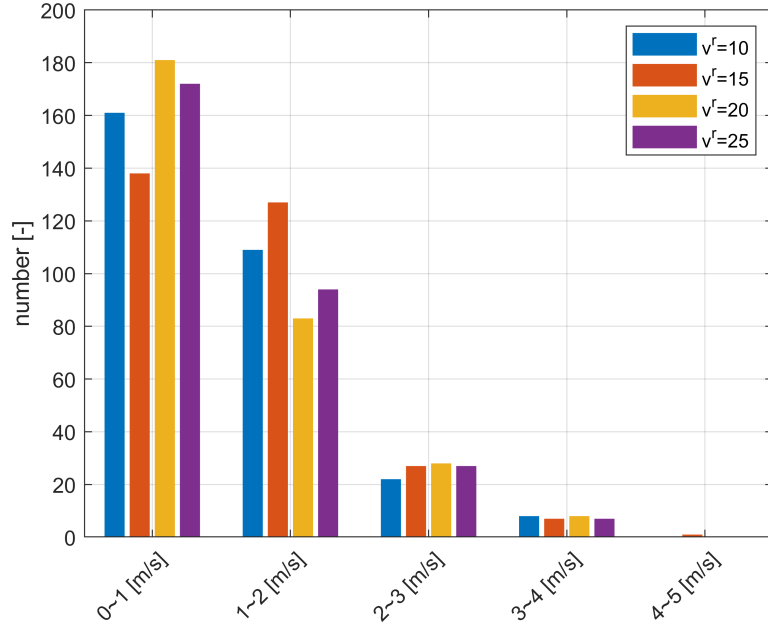


Figure 28: Distribution of average speed.

As shown in Fig. 20, the number of scheduled vehicles exhibits a rapid increase up to 300 and is followed by a gradual decline for the sequential entry and exit. The configuration $v^r = 20$ perform a special result, where the overall routing time are longer than other configurations. As shown in Fig. 21, the distribution of entering time and arriving time

for vehicles are depicted within a phase plane. Most vehicles enter the MVRP within 500 s, and the rest of vehicles enter within 1000 s to 2000 s. As shown in Fig. 22, the routing duration of DMPCs perform similar trend, all of which are around 6000 s. As shown in Fig. 23, the traveling lengths of most vehicles are similar and close around 6000 m. As shown in Fig. 24, the average speed of most vehicles are similar and within 1.5 m/s. As shown in Fig. 25, at the beginning and the end of the whole routing process, the average speed performs a high level with severe shaking, which follows the trend described in the manuscript. For the configuration $v^r = 20$, the speed is small at around 6000 s, which is quite different from other DMPCs. For this reason, the DMPC with $v^r = 20$ have a longer overall routing time. As shown in Fig. 26, for the DMPC with $v^r = 20$, the majority of vehicles complete their transportation tasks within a time frame between 8000 s and 10000 s. For the other DMPCs, the majority of vehicles complete their transportation tasks within a time frame between 6000 s and 8000 s. As shown in Fig. 27, the DMPC with $v^r = 20$ schedules more vehicles fall between 6000 m and 8000 m, while the other DMPCs schedule more vehicles between 4000 m and 6000 m. As shown in Fig. 28, for all DMPCs, most of vehicles perform their average speeds within 2 m/s. Specially, the DMPC with $v^r = 20$ have more low speed vehicles within 1 m/s and less high speed vehicles with 1-2 m/s.

Quantitatively, similar numerical indicators are introduced in this paper as Table 3 to show the difference caused by v^r .

Table 3: Quantified difference caused by v^r .

Indicators	$v^r = 10$	$v^r = 15$	$v^r = 20$	$v^r = 25$
T_{end}	9264.7	9343.6	11197.1	9159.6
T_{ave}	6206.7	5850.1	7024.5	6276.3
L_{ave}	6168.1	6184.0	6194.2	6135.2
v_{ave}	1.1566	1.2358	1.1035	1.1591

In simulations, segments are set with a speed limit from 11.1 m/s to 22.2 m/s, where most of them are set as 11.1 m/s or 16.6 m/s. Therefore, as shown in Table 3, the configuration $v^r = 15$ means the waiting vehicles are predicted to accelerate to 15 m/s while the traffic lights change Green in prediction. Such configuration is more close to the speed limits, and enables the DMPC to perform the maximum average speed 1.2358 m/s and the minimum average routing duration 5850.1 s. However, the larger v^r will introduce the more positive prediction for alternative segments $\mu_i(n+1)$ at $\mu_i(n)$. It means that for a similar alternative segments $\mu_i(n+1)$ with N_v vehicles, $v^r = 25$ will cause more probability to choose $\mu_i^*(n+1) = \mu_i(n+1)$ and $v^r = 10$ may lead the other result $\mu_i^*(n+1) \neq \mu_i(n+1)$. It can be one dimension to predict the real-world, but can not simply judge the bigger or smaller configuration will be better, which is supported by the overall results $(v^r = 20) > (v^r = 15) > (v^r = 10) > (v^r = 25)$.

3. Sensitivity analysis for θ^r :

Extending the baseline $\theta^r = 0.7$ as $\theta^r = 0.3, \theta^r = 0.5, \theta^r = 1$, the sensitivity analysis

are conducted with the 1st initial configuration in Table III. The results are shown from Figure. 29 to Figure. 37.

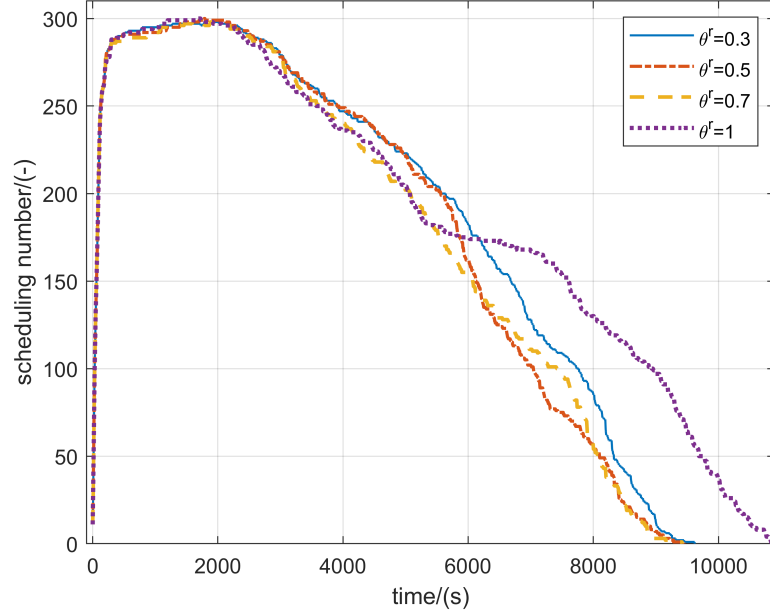


Figure 29: Scheduling vehicles in each dataframe.

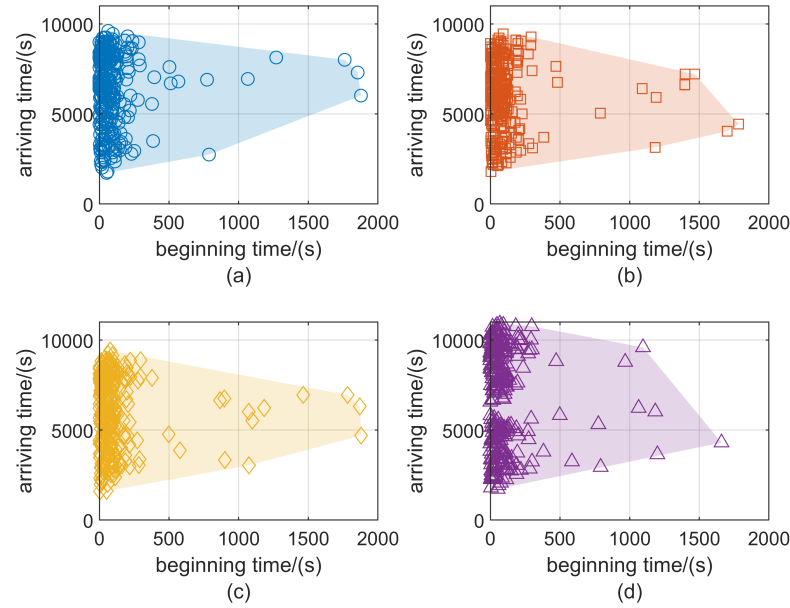


Figure 30: Entering and arriving time of vehicles: (a) $\theta^r = 0.3$ (b) $\theta^r = 0.5$ (c) $\theta^r = 0.7$ (d) $\theta^r = 1$.

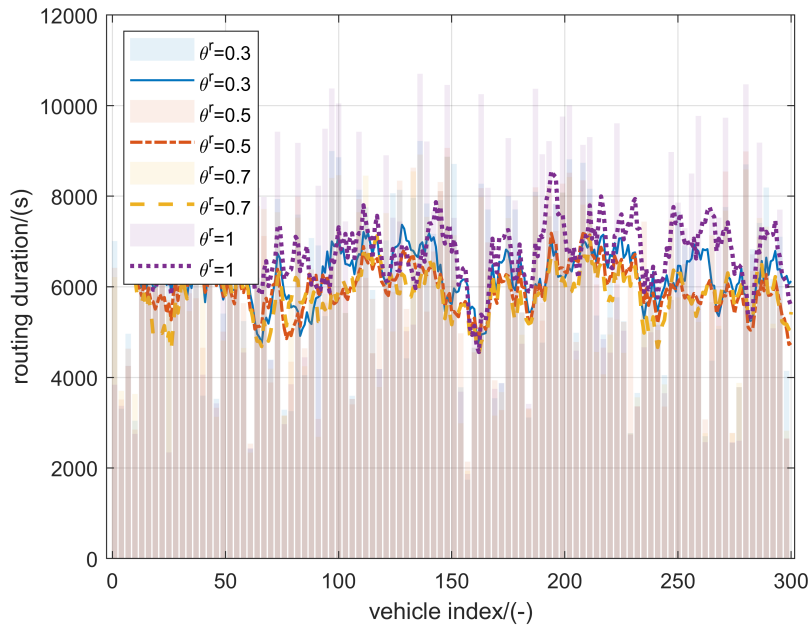


Figure 31: Routing duration of vehicles.

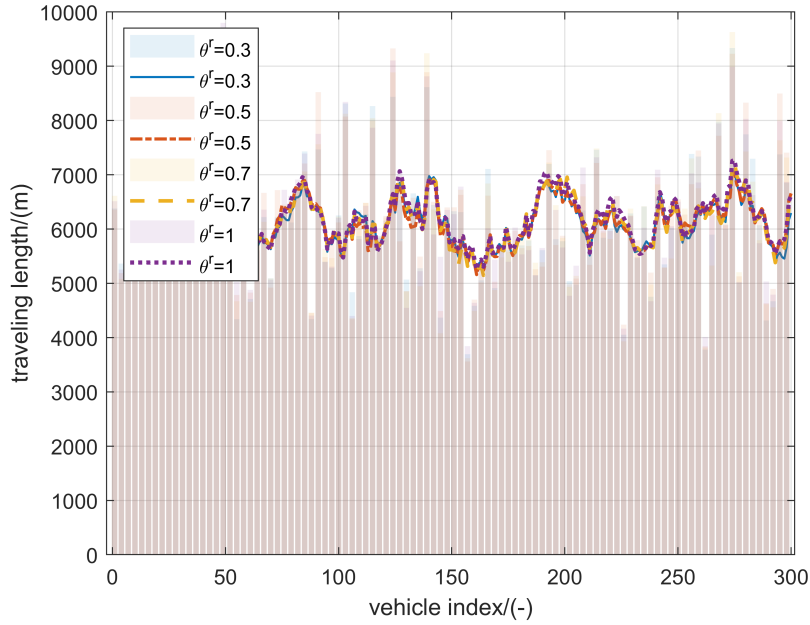


Figure 32: Traveling length of vehicles.

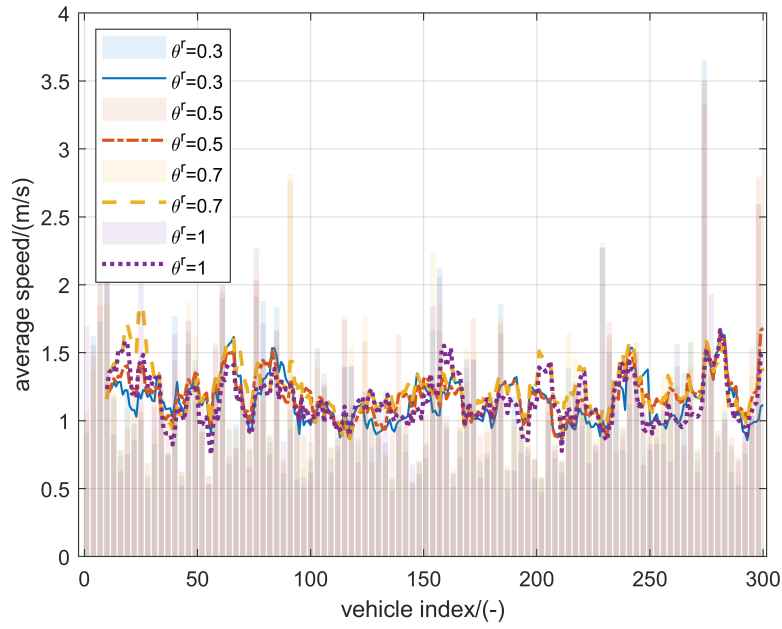


Figure 33: Average speed of vehicles.

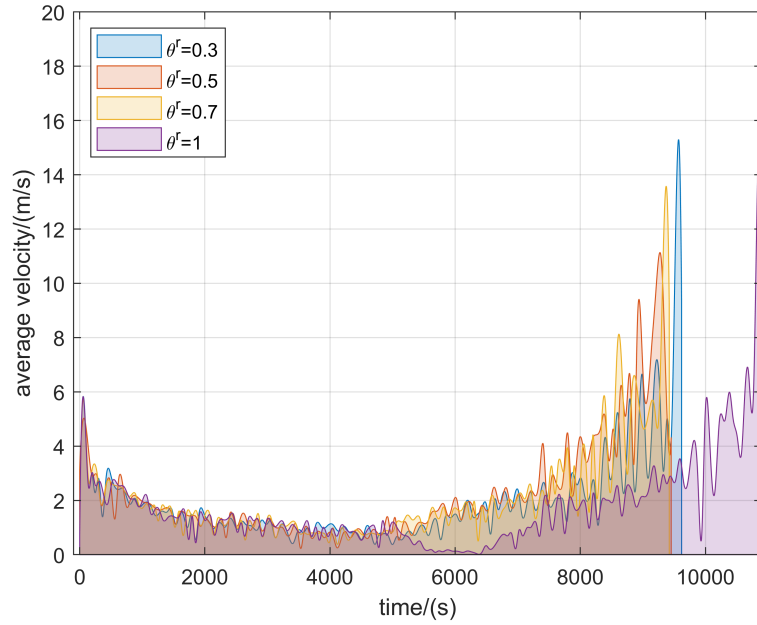


Figure 34: Average instantaneous speeds and envelopes.

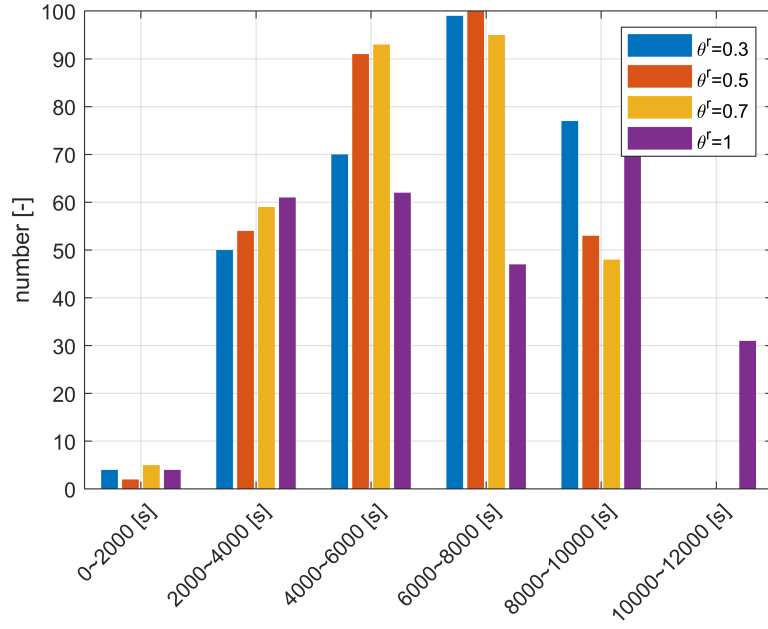


Figure 35: Distribution of routing duration.

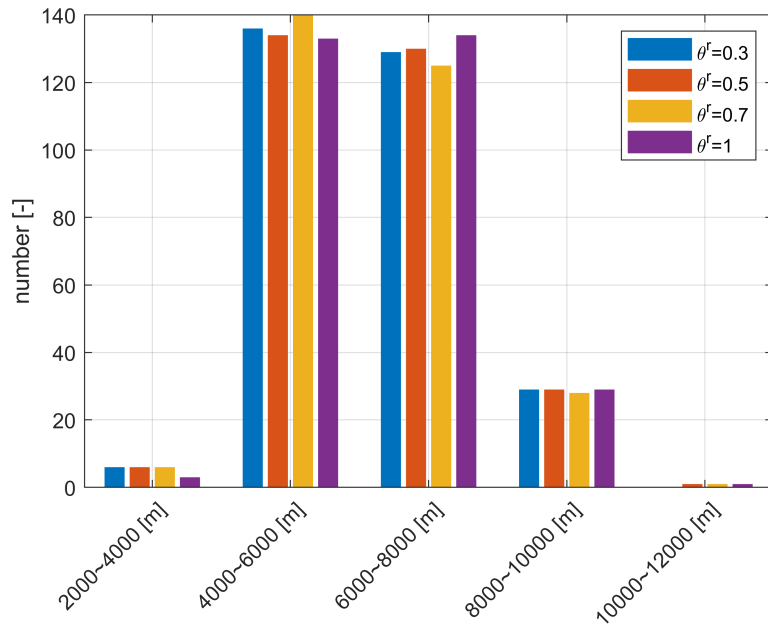


Figure 36: Distribution of traveling length.

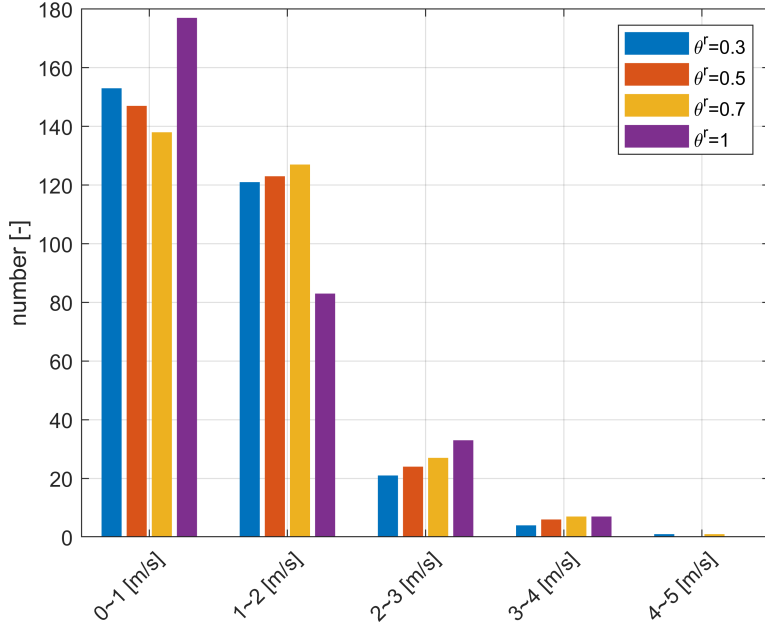


Figure 37: Distribution of average speed.

As shown in Fig. 29, the number of scheduled vehicles exhibits a rapid increase up to 300 and is followed by a gradual decline for the sequential entry and exit. The configuration $\theta^r = 1$ performs a special result, where the overall routing time are longer than other configurations. As shown in Fig. 30, the distribution of entering time and arriving time for vehicles are depicted within a phase plane. Most vehicles enter the MVRP within 500 s, and the rest of vehicles enter within 1000 s to 2000 s. As shown in Fig. 31, the routing duration of DMPCs perform similar trend, all of which are around 6000 s. As shown in Fig. 32, the traveling lengths of most vehicles are similar and close around 6000 m. As shown in Fig. 33, the average speed of most vehicles are similar and within 1.5 m/s. As shown in Fig. 34, at the beginning and the end of the whole routing process, the average speed performs a high level with severe shaking, which follows the trend described in the manuscript. For the the configuration $\theta^r = 1$, the speed is small at around 6000 s, which is quite different from other DMPCs. For this reason, the DMPC with $\theta^r = 1$ have a longer overall routing time. As shown in Fig. 35, for the DMPC with $\theta^r = 20$, the majority of vehicles complete their transportation tasks within a time frame between 8000 s and 10000 s. For the other DMPCs, the majority of vehicles complete their transportation tasks within a time frame between 6000 s and 8000 s. As shown in Fig. 36, the DMPC with $\theta^r = 1$ schedules more vehicles fall between 6000 m and 8000 m, while the other DMPCs schedule more vehicles between 4000 m and 6000 m. As shown in Fig. 37, for all DMPCs, most of vehicles perform their average speeds within 2 m/s. Specially, the DMPC with $\theta^r = 1$ have more low speed vehicles within 1 m/s and less high speed vehicles with 1-2 m/s.

Quantitatively, similar numerical indicators are introduced in this paper as Table 4 to show the difference caused by θ^r .

Table 4: Quantified difference caused by θ^r .

Indicators	$\theta^r = 0.3$	$\theta^r = 0.5$	$\theta^r = 0.7$	$\theta^r = 1$
T_{end}	9555.6	9359.6	9343.6	10841.5
T_{ave}	6235.7	5946.3	5850.1	6768.6
L_{ave}	6157.7	6177.8	6184.0	6245.3
v_{ave}	1.1421	1.1892	1.2358	1.1558

The parameter θ^r is introduced in prediction for the lane-changing vehicles to trade-off lateral lane-changing and longitudinal car-following. It is not so intuitive to understand but is a meaningful parameter, which provide another dimension of cooperative prediction. For example, imagine a lane-changing vehicle is turning into the other lane, if θ^r is big, the ego vehicle will focus on the lane-changing first and relatively ignore the car-following maneuver in prediction. Otherwise, if θ^r is small, the ego vehicle will keep following the predecessor and smoothly change lane. $\theta^r = 0.7$ is a feasible configuration from our experience of vehicle dynamic control[5, 12]. As shown in Table 4, $\theta^r = 0.7$ enables the DMPC to perform the maximum average speed 1.2358 m/s and the minimum average routing duration 5850.1 s. Similarly, it can not simply judge the bigger or smaller configuration will be better, which is supported by the overall results $(\theta^r = 0.7) > (\theta^r = 0.5) > (\theta^r = 0.3) > (\theta^r = 1)$.

4. Sensitivity analysis for k_Q :

Extending the baseline $k_Q = 2$ as $k_Q = 1, k_Q = 3$, the sensitivity analysis are conducted with the 1st initial configuration in Table III. The results are shown from Figure. 38 to Figure. 46.

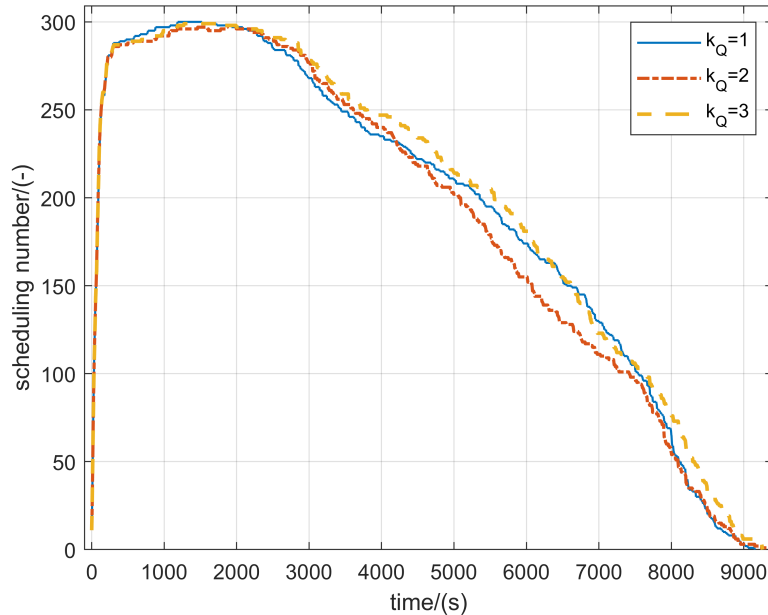


Figure 38: Scheduling vehicles in each dataframe.

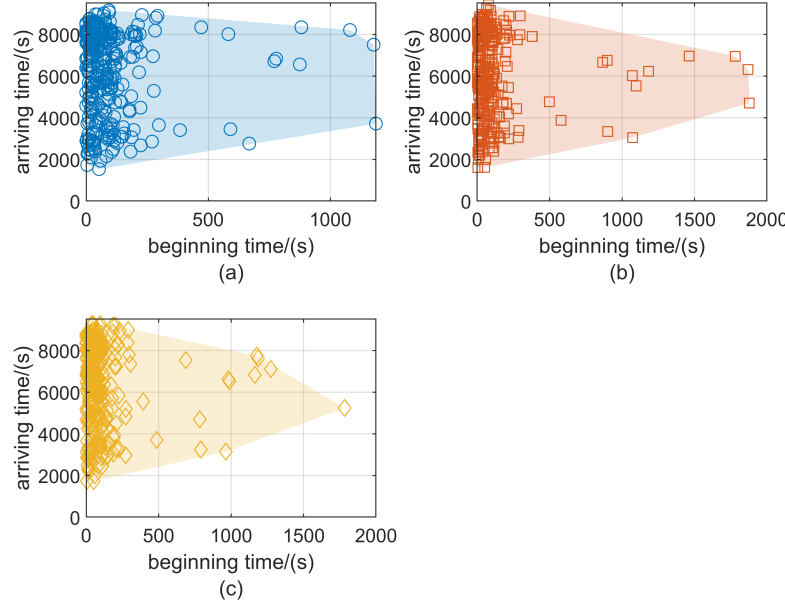


Figure 39: Entering and arriving time of vehicles: (a) $K_Q = 1$ (b) $K_Q = 2$ (c) $K_Q = 3$.

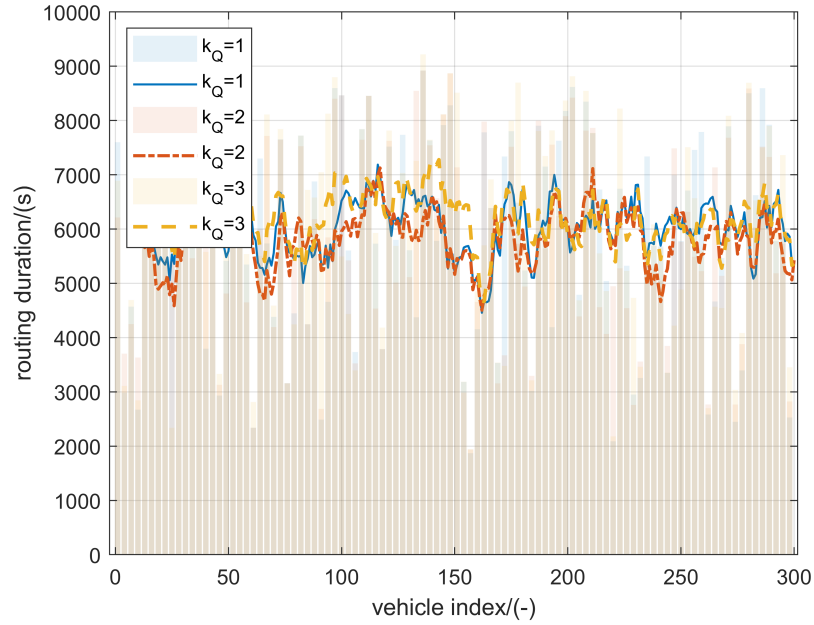


Figure 40: Routing duration of vehicles.

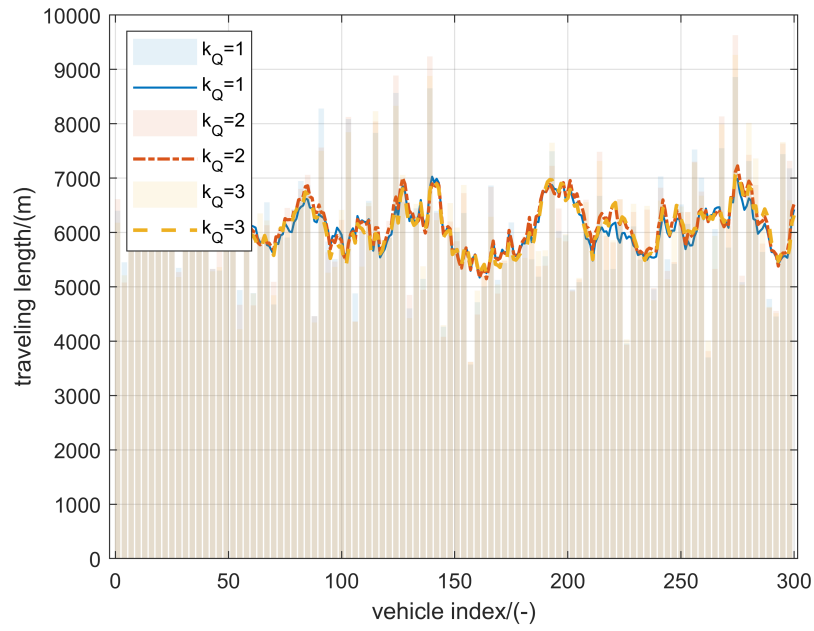


Figure 41: Traveling length of vehicles.

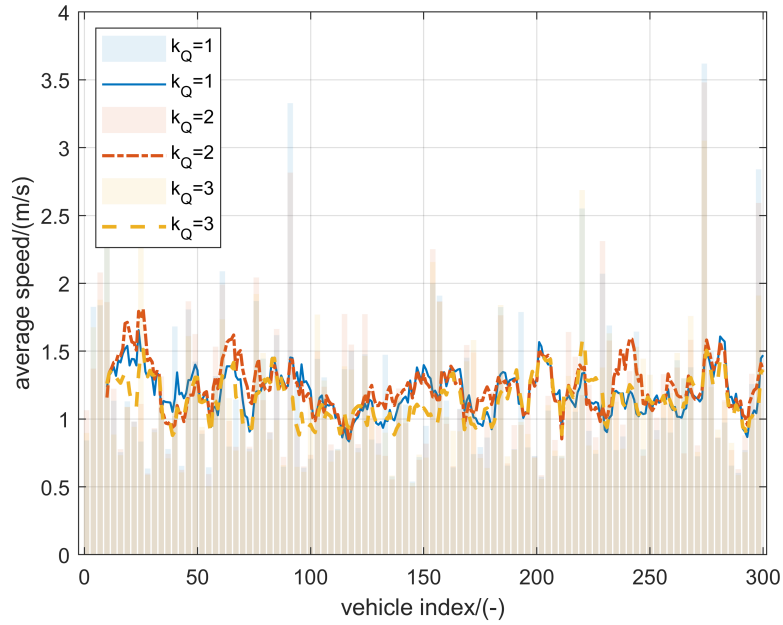


Figure 42: Average speed of vehicles.

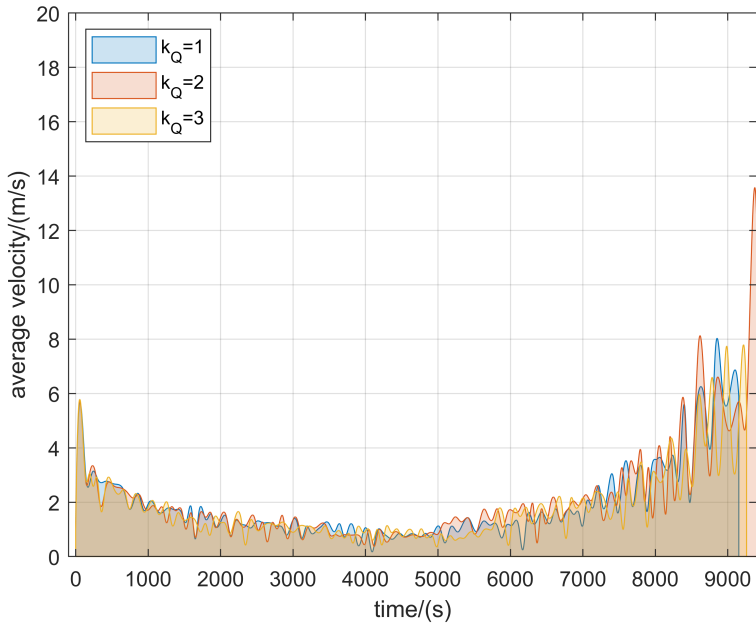


Figure 43: Average instantaneous speeds and envelopes.

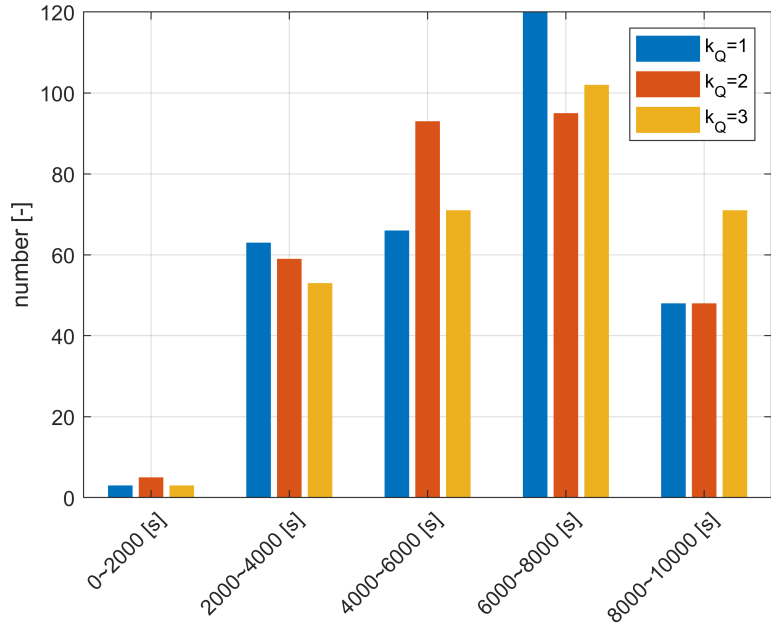


Figure 44: Distribution of routing duration.

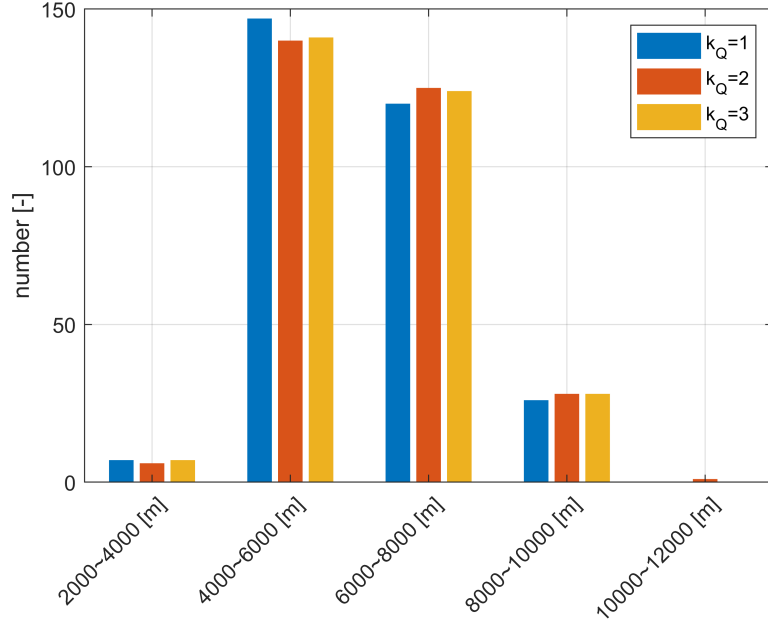


Figure 45: Distribution of traveling length.

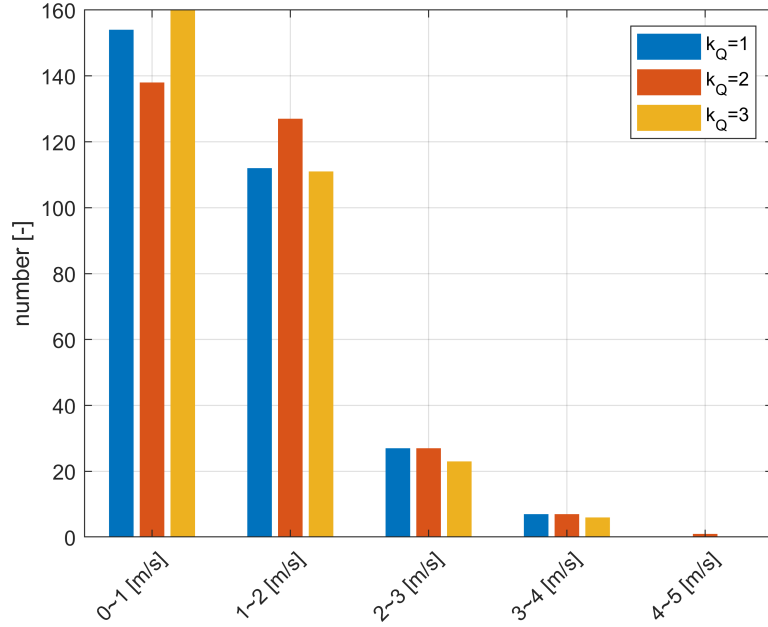


Figure 46: Distribution of average speed.

As shown in Fig. 38, the number of scheduled vehicles exhibits a rapid increase up to 300 and is followed by a gradual decline for the sequential entry and exit. As shown in Fig. 39, the distribution of entering time and arriving time for vehicles are depicted within a phase plane. Most vehicles enter the MVRP within 500 s, and the rest of

vehicles enter within 1000 s to 2000 s. As shown in Fig. 40, the routing duration of DMPCs perform similar trend, all of which are around 6000 s. As shown in Fig. 41, the traveling lengths of most vehicles are similar and close around 6000 m. As shown in Fig. 42, the average speed of most vehicles are similar and within 1.5 m/s. As shown in Fig. 43, at the beginning and the end of the whole routing process, the average speed performs a high level with severe shaking, which follows the trend described in the manuscript. As shown in Fig. 44, for all DMPCs, the majority of vehicles complete their transportation tasks within a time frame between 6000 s and 8000 s. As shown in Fig. 45, all DMPCs schedule most vehicles between 4000 m and 6000 m. As shown in Fig. 46, for all DMPCs, most of vehicles perform their average speeds within 2 m/s. By comparison, the DMPC with $k_Q = 2$ have less low speed vehicles within 1 m/s and more high speed vehicles with 1-2 m/s.

Quantitatively, similar numerical indicators are introduced in this paper as Table 5 to show the difference caused by k_Q .

Table 5: Quantified difference caused by k_Q .

Indicators	$k_Q = 1$	$k_Q = 2$	$k_Q = 3$
T_{end}	9059.4	9343.6	9218.6
T_{ave}	6006.8	5850.1	6166.6
L_{ave}	6115.4	6184.0	6128.9
v_{ave}	1.1987	1.2358	1.1498

The parameter k_Q is introduced in prediction for vehicles to choose their target lanes. It is not so intuitive to understand but is a meaningful parameter, which provide another dimension of cooperative prediction. For example, imagine a vehicle will turn into segment $\mu_i(n+1)$ from the current segment $\mu_i(n)$ with available connections. To achieve the traveling, there will be several alternative lanes and k_Q, k_C will give the trend for the choice of the ego vehicle. If k_Q is relatively big, the ego vehicle will be predicted to choose the lane with minimum number of vehicles. Otherwise, the ego vehicle will be predicted to choose a conflict-free lane, which gives a huge space for the ego vehicle to change lane but may be chosen by many surrounding vehicles. $k_Q = 2$ is a feasible configuration based on the manual trial and error. As shown in Table 5, $k_Q = 2$ enables the DMPC to perform the maximum average speed 1.2358 m/s and the minimum average routing duration 5850.1 s. Similarly, it can not simply judge the bigger or smaller configuration will be better, which is supported by the overall results $(k_Q = 1) > (k_Q = 3) > (k_Q = 2)$.

5. Sensitivity analysis for k_C :

Extending the baseline $k_Q = 2$ as $k_Q = 1, k_Q = 3$, the sensitivity analysis are conducted with the 1st initial configuration in Table III. The results are shown from Figure. 47 to Figure. 55.

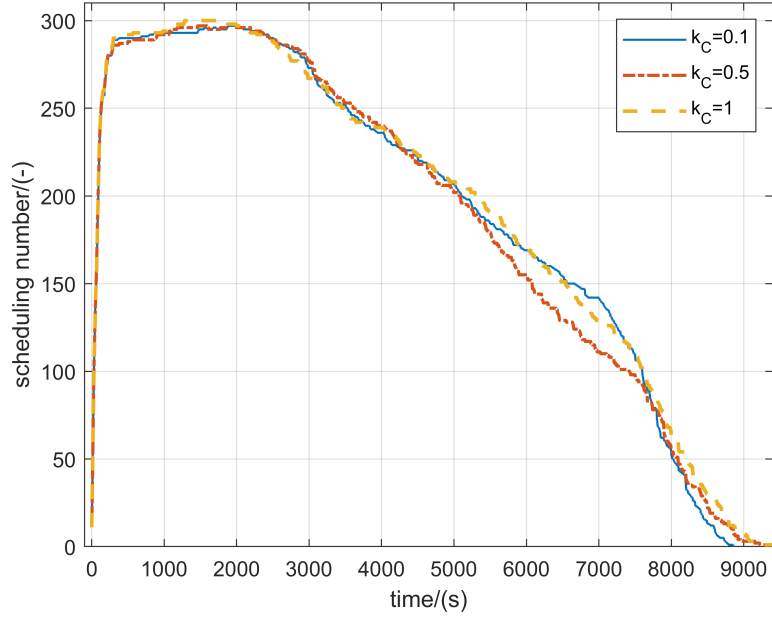


Figure 47: Scheduling vehicles in each dataframe.

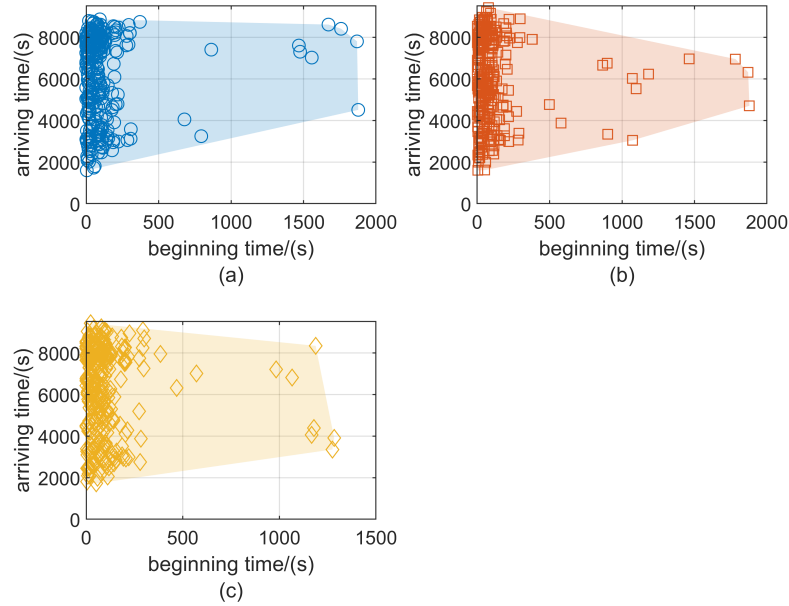


Figure 48: Entering and arriving time of vehicles: (a) $K_Q = 1$ (b) $K_Q = 2$ (c) $K_Q = 3$.

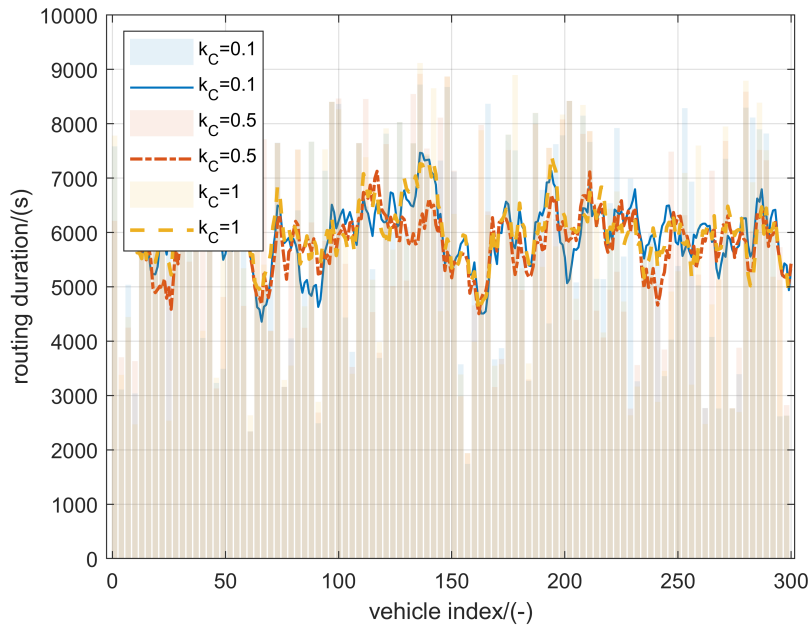


Figure 49: Routing duration of vehicles.

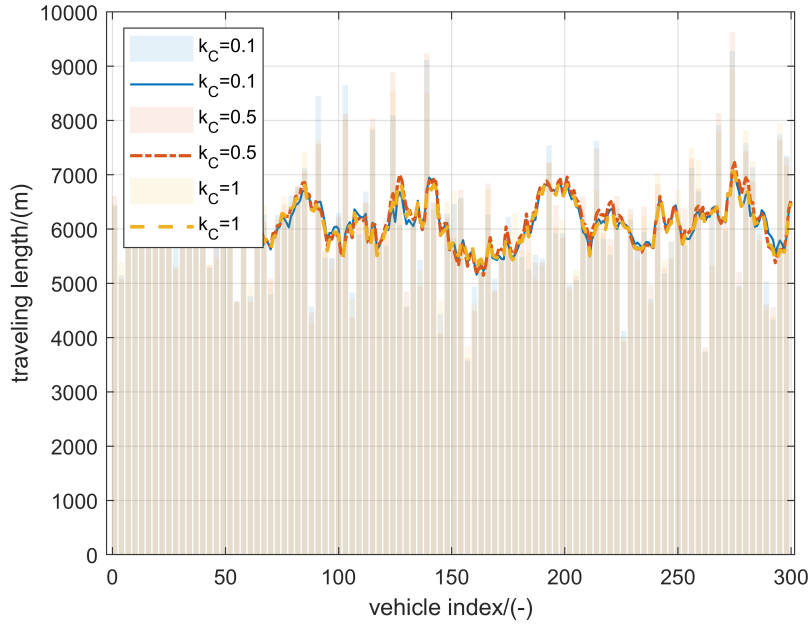


Figure 50: Traveling length of vehicles.

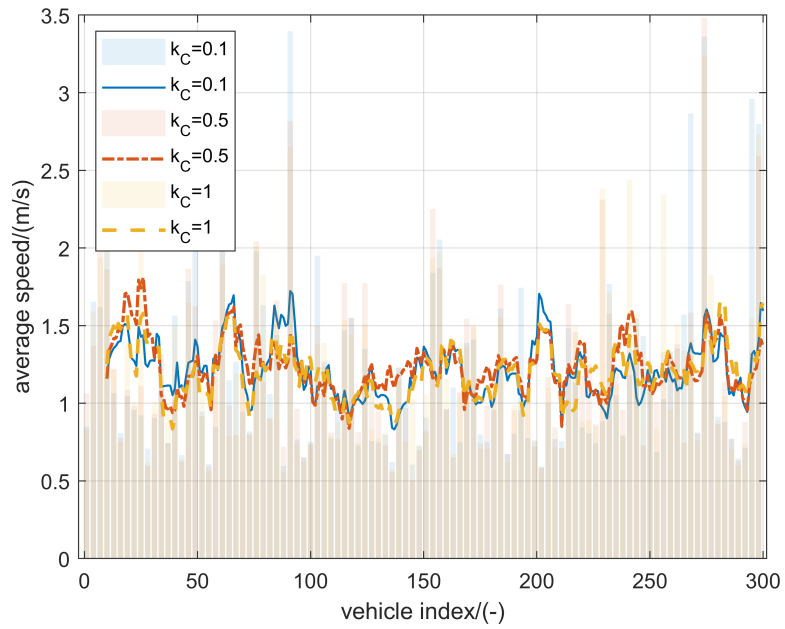


Figure 51: Average speed of vehicles.

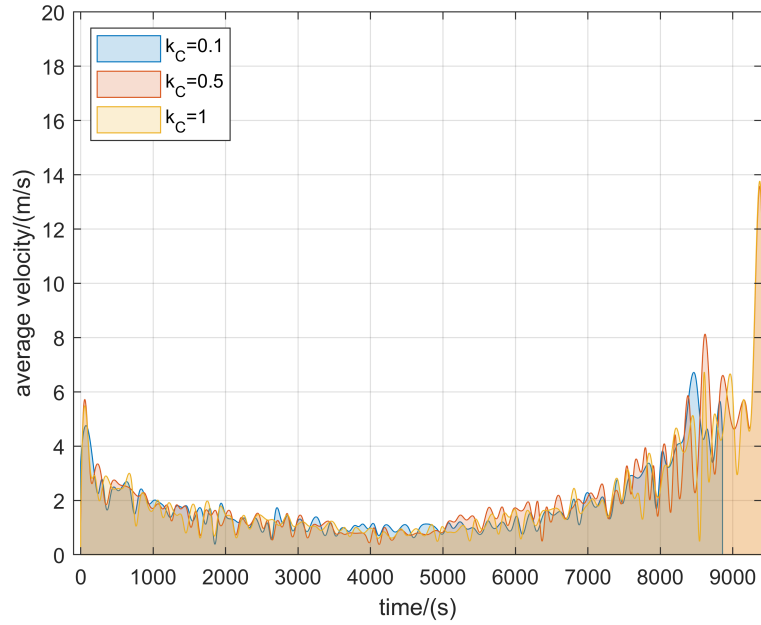


Figure 52: Average instantaneous speeds and envelopes.

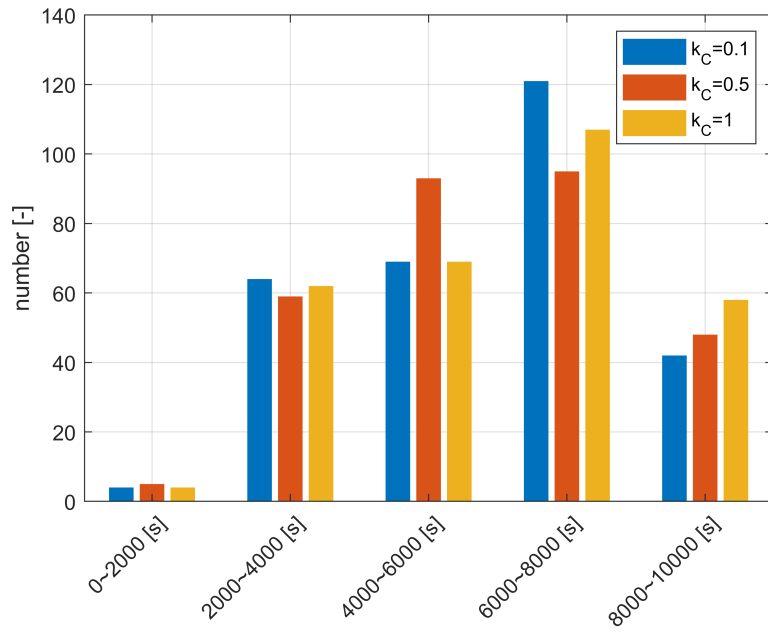


Figure 53: Distribution of routing duration.

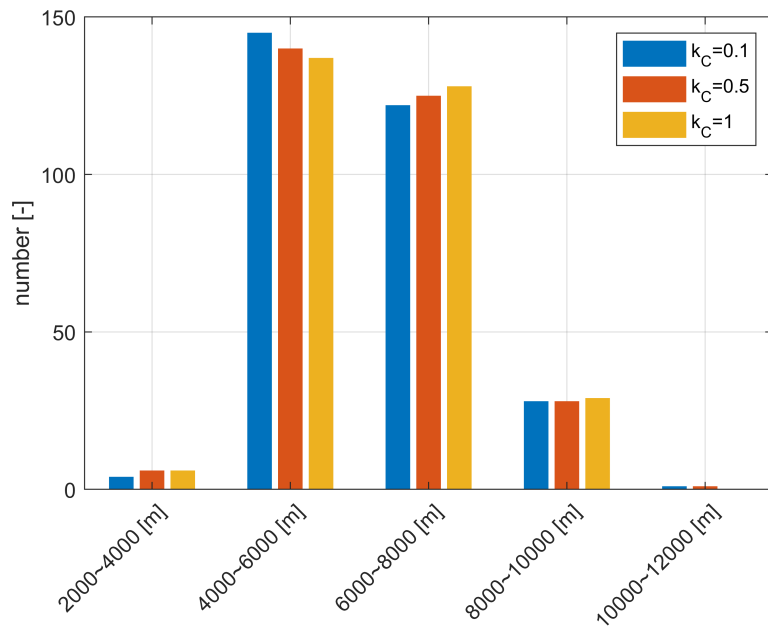


Figure 54: Distribution of traveling length.

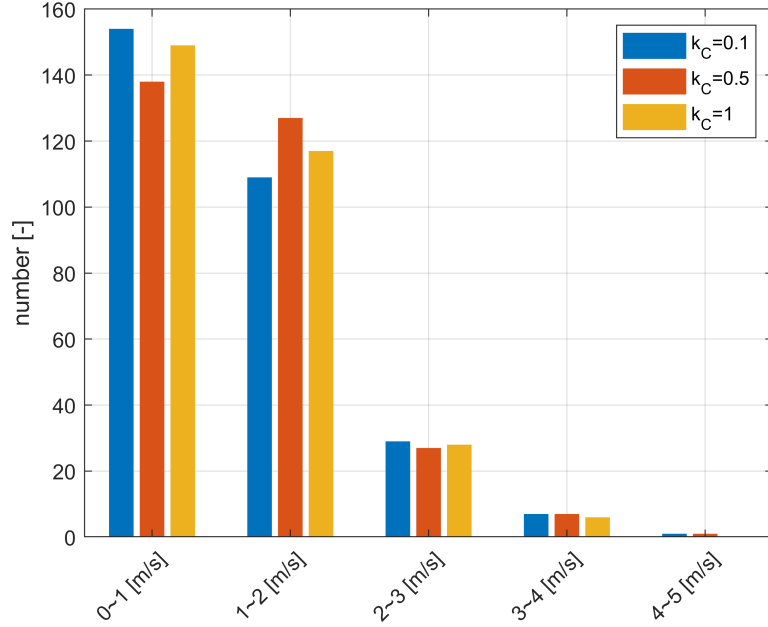


Figure 55: Distribution of average speed.

As shown in Fig. 47, the number of scheduled vehicles exhibits a rapid increase up to 300 and is followed by a gradual decline for the sequential entry and exit. As shown in Fig. 48, the distribution of entering time and arriving time for vehicles are depicted within a phase plane. Most vehicles enter the MVRP within 500 s, and the rest of vehicles enter within 1000 s to 2000 s. As shown in Fig. 49, the routing duration of DMPCs perform similar trend, all of which are around 6000 s. As shown in Fig. 50, the traveling lengths of most vehicles are similar and close around 6000 m. As shown in Fig. 51, the average speed of most vehicles are similar and within 1.5 m/s. As shown in Fig. 52, at the beginning and the end of the whole routing process, the average speed performs a high level with severe shaking, which follows the trend described in the manuscript. As shown in Fig. 53, for all DMPCs, the majority of vehicles complete their transportation tasks within a time frame between 6000 s and 8000 s. By comparison, the DMPC with $k_C = 0.5$ have more vehicles within 4000-6000 s. As shown in Fig. 54, all DMPCs schedule most vehicles between 4000 m and 6000 m. As shown in Fig. 54, for all DMPCs, most of vehicles perform their average speeds within 2 m/s. By comparison, the DMPC with $k_C = 0.5$ have less low speed vehicles within 1 m/s and more high speed vehicles with 1-2 m/s.

Quantitatively, similar numerical indicators are introduced in this paper as Table 6 to show the difference caused by k_C .

Similar to k_Q , k_C is introduced in prediction for vehicles to choose their target lanes. As a compensation of k_Q , k_C provide a prediction for how many efforts the vehicles will take to avoid lane-changing-induced conflicts. Imagine a vehicle will turn into segment $\mu_i(n+1)$ from the current segment $\mu_i(n)$ with available connections. To achieve the traveling, there will be several alternative lanes and k_Q, k_C will give the trend for the

Table 6: Quantified difference caused by k_C .

Indicators	$k_C = 0.1$	$k_C = 0.5$	$k_C = 1$
T_{end}	9764.6	9343.6	9398.7
T_{ave}	5950.4	5850.1	6024.2
L_{ave}	6146.6	6184.0	6149.6
v_{ave}	1.2193	1.2358	1.2096

choice of the ego vehicle. If k_C is relatively big, the ego vehicle will be predicted to choose the conflict-free lane, otherwise, they will be predicted to choose the shortest queued lane. $k_C = 0.5$ is a feasible configuration based on the manual trial and error. As shown in Table 5, $k_C = 0.5$ enables the DMPC to perform the maximum average speed 1.2358 m/s and the minimum average routing duration 5850.1 s. Similarly, it can not simply judge the bigger or smaller configuration will be better, which is supported by the overall results $(k_C = 0.1) > (k_C = 0.5) > (k_C = 1)$.

Primary results about computational efficiency

1. Recorded running time: For the computing cost of the proposed algorithm, we provide some results about this as Table 7. The computing time is a significant indicator for on-

Table 7: Running time of various initialization.

Initialization Index	Solved Number of DMPCs	Average Time of Each DMPC
1	17725	1.1127
2	17558	1.0995
3	17576	1.1606
4	17668	1.2100
5	17584	1.1041

line planner. However, on the one hand, without an open-source code for the compared method, we can not conclude the improvement of our methods in computing speed. On the other hand, we have not made much efforts on computing improving in our work, which makes the main contribution is not so related to the computing cost. For example, the solution of optimization (16) in this paper is based on sampling and traversal, which is the simplest solving method but bring a negative influence for running time.